Asian Journal of Chemistry Vol. 21, No. 3 (2009), 2198-2206

Preparation and Characterization of (SBA-15)-Rhodamine B Host-Guest Nanocomposite Material

QING-ZHOU ZHAI* and DONG YANG
Research Center for Nanotechnology, South Campus,Changchun University of Science and Technology, 7186 Weixing Road, Changchun 130022, P.R. China
E-mail: zhaiqingzhou@sohu.com; zhaiqingzhou@hotmail.com
Fax: (86)(431)85383815; Tel: (86)(431)85583118

In the present study, SBA-15 molecular sieve was prepared by a hydrothermal method using the triblock copolymer poly (ethylene glycol)-block-poly(propyl glycol)-block-poly (ethylene glycol) ($EG_{20}PG_{40}EG_{20}$) as a template and tetraethyl orthosilicate as silica source. Rhodamine B (RhB) nanoclusters have been successfully prepared in the channels of the SBA-15 molecular sieve host and a (SBA-15)-RhB host-guest nanocomposite material was prepared by liquid grafting method. By means of chemical analysis, powder X-ray diffraction, infrared spectroscopy, low-temperature nitrogen adsorption-desorption technique, solid state diffuse reflectance absorption spectroscopy and luminescence studies, the host-guest nanocomposite material was characterized. The results suggested that the guest RhB was successfully encapsulated in the channels of the host SBA-15 molecular sieve and the frameworks of the molecular sieve in the prepared composite materials were retained and highly ordered. The prepared host-guest nanocomposite material (SBA-15)-RhB shows luminescence and it may used as luminescence material.

Key Words: Nanocomposite material, SBA-15 mesoporous molecular sieve host, Rhodamine B guest, Nanocluster.

INTRODUCTION

Molecular sieves are a kind of porous materials, which can be used as adsorbent, catalyst, *etc*. The discovery of mesoporous molecular sieve[1,2] has stimulated wide interest for its potential applications in various fields, such as catalysis, optoelectronic devices, host-guest materials and carrier systems for controlled-release delivery of drugs[3-8]. Mesoporous molecular sieves are ideal hosts for producing nanostructures of organic and inorganic materials. These host-guest composite materials are potentially new functional materials in electric transport, optical switches, nonlinear optics and lasers[9-12]. Some researchers discussed to find out appropriate conditions for efficient incorporation of dyes into molecular sieves[13-15]. Recently, the different application of dye-containing molecular sieves to photochromic or optic sensors is of great interest[16]. Molecular sieves improve the monomeric dispersion and fixation of dye guests, reduce rotational relaxation of excited states of dyes, which is the

main source of non-radiative energy loss. They exhibit superior physical properties like low thermal expansion, low strain birefringence, or low non-linear refractive index[17]. The host-guest materials based on dyes loaded mesoporous substances will exhibit particular advantages for optical function in optical and chemical sensors[18-22]. SBA-15 molecular sieve is the mesoporous molecular sieve with largest pore size. It has highly ordered hexagonally arranged channels, thick walls, adjustable pore size from 5 to 30 nm and high hydrothermal and thermal stability[23,24]. Compared with other mesoporous molecular sieves, SBA-15 possesses larger pore sizes, thicker walls and higher hydrothermal stability[25-28]. In contrast to other mesoporous materials such as MCM-41, SBA-15 may hopefully become a better host for the formation of nanostructures because its larger pores and thicker wall can provide stronger confinement on guest and its larger pores are more suitable to be a good template for preparing quantum dots and nano quantum wires. Rhodamine B ($C_{28}H_{31}N_2O_3Cl$) is a member in the family of fluorone dyes compounds. It is used as a dye and as a dye laser gain medium. The chemical structure of rhodamine B is shown in Fig. 1. In the present paper, rhodamine B was chosen as a guest to be incorporated into the SBA-15 molecular sieve host by liquid grafting method. A series of characterization techniques, chemical analysis, power X-ray diffraction, Fourier transform infrared spectroscopy, low temperature nitrogen adsorption-desorption technique, solid diffuse reflectance absorption spectroscopy and photoluminescence studies were used to characterize the prepared host-gust nanocomposite material. The prepared host-guest nanocomposite material may be applied to the field of luminescence materials.

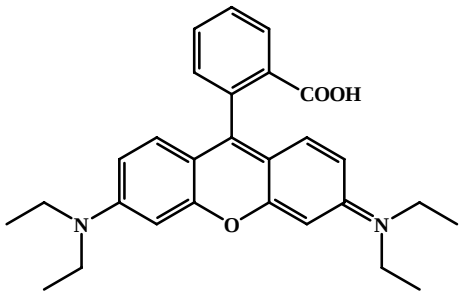

Fig. 1. Chemical structure of rhodamine B

EXPERIMENTAL

Triblock copolymer poly(ethyleneglycol)-block-poly(propylene glycol)-block-poly(ethylene glycol)(average relative molecular mass 5800, Fluka, template). Tetraethyl orthosilicate (TEOS, Shanghai Chemical Co., Ltd.). Rhodamine B ($C_{28}H_{31}N_2O_3Cl$, Shanghai Third Reagent Plant): 1.0×10^{-4} mol/L. Hydrochloric acid: 2.0 mol/L. All reagents used were analytical grade. Doubly deionized water was used in the experiments.

Sample preparation: The SBA-15 molecular sieve was prepared under a strong acidic condition by using triblock copolymer, poly(ethylene glycol)-block-poly(propylene glycol)-block-poly(ethylene glycol) as the template. The composition was as follows: 2.0 g of amphiphilic triblock copolymer, poly(ethylene glycol)-block-poly(propylene glycol)-block-poly(ethylene glycol) was dispersed in 15.0 g of deionized water and 60.0 g of 2.0 mol/L hydrochloric acid solution while stirring, followed by the addition of 4.25 g of tetraethyl orthosilicate to the homogeneous solution with stirring. This gel mixture was continuously stirred at 40 ºC for 24 h and finally crystallized in a telflon-lined autoclave at 100 ºC for 2 d. After crystallization, the solid product was filtered, washed with deionized water and dried in air at room temperature. The material was calcined in static air at 550 ºC for 24 h to decompose the triblock copolymer and obtain a white powder (SBA-15). This white powder was used as host material to produce the host-guest nanocomposite material (SBA-15)-RhB *via* the following route. 0.300 g of the prepared SBA-15 molecular sieve was placed in 60 mL of 1.0×10^{-4} mol/L rhodamine B aqueous solution at room temperature for 48 h with stirring. The product was then filtrated and washed using doubly deionized water until no free rhodamine B could be detected. Finally, the product was dried at 60 ºC for 6 h to obtain the assembly product, designed as (SBA-15)-RhB. The size of the (SBA-15)-RhB sample was determined to be 150 nm by scanning electric microscopy (images not shown).

Characterization: Chemical analysis was carried out by siliconantimomolybdate heteropoly blue photometry[29]. X-ray diffraction (XRD) patterns were collected with a diffractometer (D5005, Siemens, Germany) with CuK_α radiation operation at 30 kV and 20 mA for small angles (0.4°~10.0°) with step size of 0.02° and a step time of 2 s. Fourier transform infrared spectra (FTIR) were recorded on a Nicolet 5DX-FTIR spectrometer, using the potassium bromide wafer technique. Adsorption-desorption study of nitrogen was performed on a Micromeritics ASAP2010M volumetric adsorption analyzer at 77K. A sample was degassed in vacuum at 573 K for 12 h before measurement. Surface area was calculated based on the BET (Brunner-Emmett-Teller) method[30], while pore size distribution was computed using the BJH (Barrett-Joyner-Halenda) method[31]. Solid state diffuse reflectance absorption spectra were obtained with a Cary 500 ultraviolet-visible-near infrared spectrophotometer (Varian, USA). Luminescence studies were performed on a SPEX-FL-2T-2(SPEX, USA) fluorescence spectrophotometer at a room temperature of 25 ºC.

RESULTS AND DISCUSSION

The content of the SBA-15 molecular sieve in the prepared host-guest composite material was determined by siliconantimomolybdate heteropoly blue photometry. The content of the RhB was obtained by the difference subtraction. The results of chemical analysis show that the molecular formula in terms of the content is $C_{28}H_{31}N_2O_{51}ClSi_{24}$. This indicates that the guest RhB has already been incorporated into the prepared nanocomposite material.

The small-angle XRD patterns of the samples are shown in Fig. 2. One major peak at 0.9° together with 3 additional small peaks of the sample SBA-15 can be observed which is characteristic of SBA-15 and is in good agreement with those reported in the literature[23,24]. The 4 well-resolved peaks are indexed as (100), (110), (200) and (210) reflections associated with p6mm hexagonal symmetry. The X-ray diffraction pattern of the (SBA-15)-RhB sample shows 3 peaks that are corresponding to the (100), (110) and (200), respectively. The results suggest that the hexagonal pore of SBA-15 is retained in the (SBA-15)-RhB sample after being incorporated with the RhB. The well-resolved peaks indicate that samples possess a long-range-ordered structure. However, the facts that for the curve of the (SBA-15)-RhB sample the 4th peak corresponding to the (210) is disappeared and the intensity of the other 3 peaks decreases show that RhB causes the reduction of peak intensity of diffraction. The crystal face spacing d_{100} obtained and the calculated unit cell parameter a_0, which show the effect of the incorporation of the RhB on the mesoporous structure, are listed in Table-1.

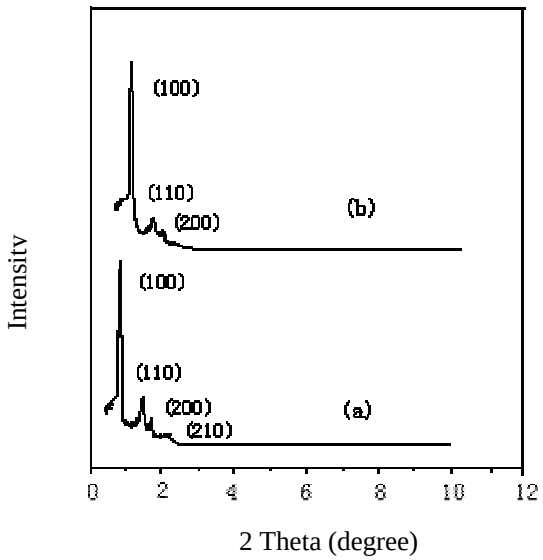

Fig. 2. XRD patterns of the samples: (a) SBA-15;(b) (SBA-15)-RhB

TABLE-1
PORE STRUCTURE PARAMETERS OF THE SAMPLES

Sample	d_{100} (nm)	a_0[a] (nm)	BET surface area ($m^2 g^{-1}$)	Pore volume[b] ($cm^3 g^{-1}$)	Pore size[c] (nm)	Wall thickness[d] (nm)
SBA-15	9.56	11.04	662	1.14	6.77	4.27
(SBA-15)-RhB	10.63	12.28	620	0.97	6.33	5.95

[a] $a_0 = \frac{2}{\sqrt{3}} d_{100}$; [b] BJH adsorption cumulative volume of pores; [c] Pore size calculated from the adsorption branch; [d] Wall thickness calculated by (a_0 - pore size).

Fig. 3 shows the FTIR spectra of the SBA-15, (SBA-15)-RhB and RhB samples. For the spectrum of the SBA-15 (Curve A), there are several characteristic peaks. The peak at 1092 cm^{-1} can be attributed to the asymmetric stretching vibration of the Si-O-Si. The peak of 965 cm^{-1} is assigned to the bending vibration of the Si-OH. The peaks at 802 and 466 cm^{-1} correspond to the symmetric stretching vibration of the Si-O-Si and the bending vibration of the Si-O-Si, respectively. In Fig. 3, the spectrum of the (SBA-15)-RhB (Curve B) is almost the same as that of the SBA-15 and dose not possess the characteristic peaks of the RhB. The FTIR spectra results show that the framework of the molecular sieve in the prepared (SBA-15)-RhB sample was retained after the molecules of RhB were introduced into the host and no collected RhB existed. Also, the RhB dispersed in the channels of the SBA-15 in a homogeneous way.

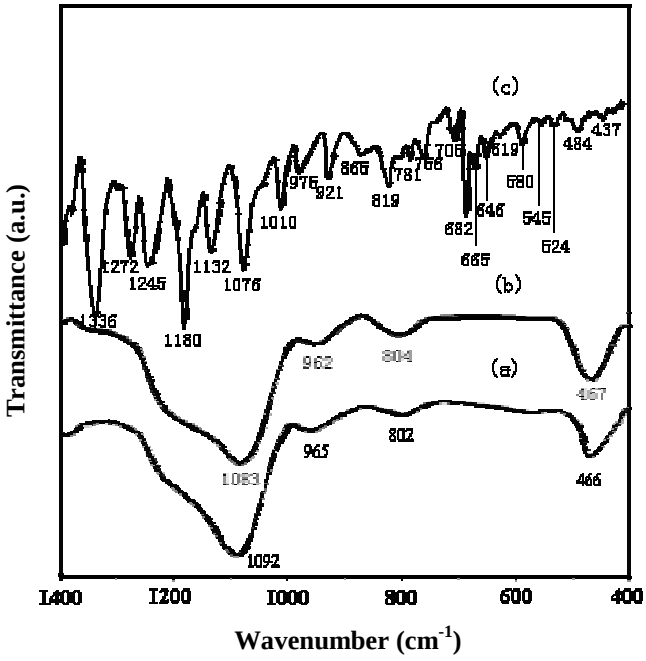

Fig. 3. Infrared spectra of the samples: (a) SBA-15; (b) (SBA-15)-RhB; (c) RhB

To characterize the change in pore features of the SBA-15 before and after the inclusion of RhB in the molecular sieve, low temperature N_2 adsorption-desorption isotherms were used to characterize the samples. The isotherm for the SBA-15 sample (Curve A) is similar to those reported earlier[23,24]. Consistent with above XRD results, (SBA-15)-RhB sample also gives similar isotherm curve to that of SBA-15, which reflects the maintenance of ordered mesostrures in the prepared (SBA-15)-RhB. According to the IUPAC classification[32], their irreversible type LangmuirIV adsorption isotherms with a H1 hysteresis loop indicate that all samples

have mesoporous channels and a narrow pore size distribution. In each isotherm, the adsorption inflection at the relative pressure from 0.6 to 0.8 is associated with capillary condensation taking place in the mesopores and its steepness reveals the uniformity of mesopore size. In addition, the position of the inflection point is closely related to the mesopore size. As shown in Fig. 4, for (SBA-15)-RhB sample there are slight shifts of the inflection point towards the low pressure region compared with that of SBA-15. The observed behaviour proves that RhB has been successfully contained into the pores of the SBA-15.

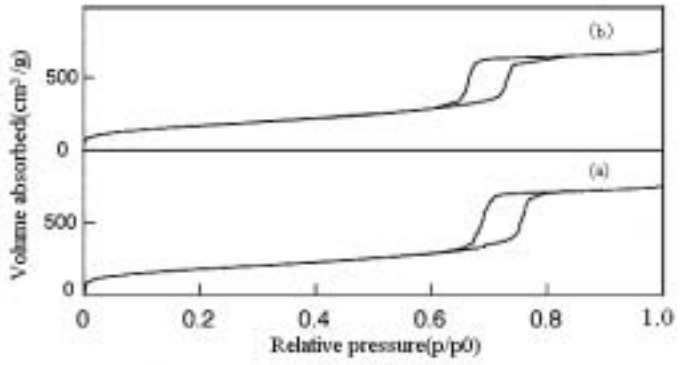

Fig. 4. Low temperature nitrogen adsorption-desorption isotherms: (a) SBA-15; (b) (SBA-15)-RhB

The pore size distributions for the samples are shown in Fig. 5 and the average pore sizes corresponding to their maxima are listed in Table-1. The pore size distributions exhibit sharp shape, suggesting that the samples possess uniform pore sizes. The corresponding pore structural parameters calculated from nitrogen adsorption-desorption isotherms and the XRD data are given in Table-1. It displays a decrease in average pore sizes, pore volumes and the BET specific surface area. This implies that most of the pores are filled up by the RhB. At the same time it can be observed from Table-1 that the unit cell parameter (a_0), crystal face spacing (d_{100}) and wall thickness of the (SBA-15)-RhB sample are all increased compared with those of SBA-15 since some molecules of the RhB were adhered to the walls of the SBA-15 in the host-guest nanocomposite materials.

The UV-vis solid diffuse reflection absorption spectra of the SBA-15, RhB and (SBA-15)-RhB samples are shown in Fig. 6. It is clearly observed that over the wavelength range, the SBA-15 molecular sieve barely has adsorption (Curve A) and the spectrum of (SBA-15)-RhB (Curve B) has two absorption bands at 356 and 537 nm. Blue-shifts take place relative to the adsorption bands of the RhB at 431 and 611 nm (Curve C). The results verify the existence of the RhB in the channels of the SBA-15. The massive blue-shift can be explained in terms of the quantum size effects of channels of the SBA-15. This also further proves that the RhB has already successfully encapsulated in the channels of the SBA-15.

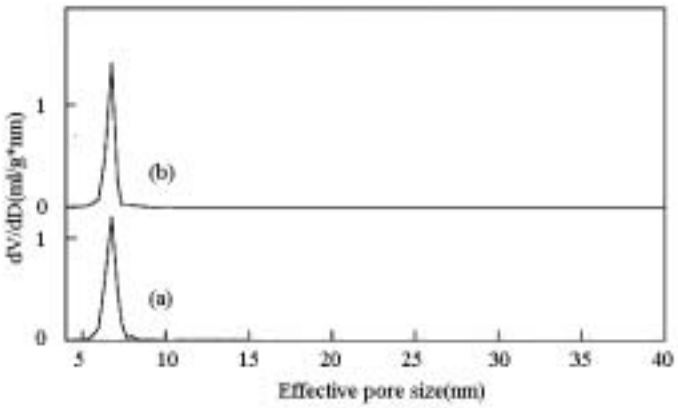

Fig. 5. Pore size distribution patterns of the samples: (a) (SBA-15)-RhB;(b) SBA-15

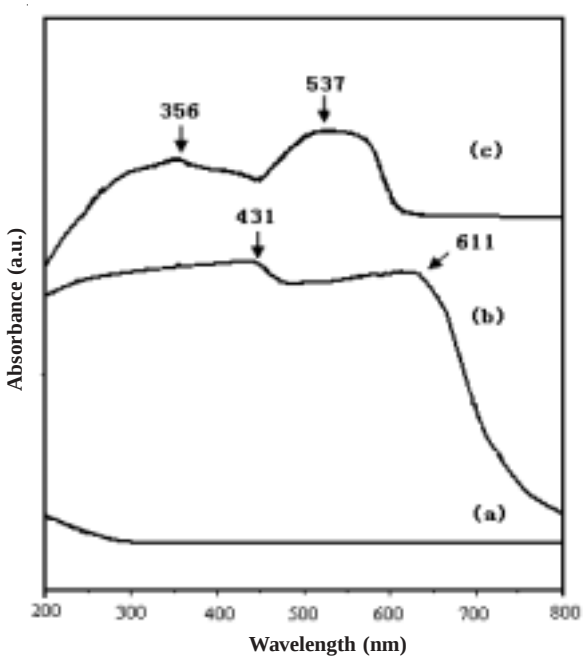

Fig. 6. Solid state diffuse reflectance absorption spectra of the samples: (a) SBA-15; (b) RhB; (c) (SBA-15)-RhB

Neither the SBA-15 nor the RhB has luminescence. However, the (SBA-15)-RhB sample shows photoluminescence (Fig. 7) at room temperature. Fig. 7 shows that the emission wavelength corresponding to the excitation of 356 nm is at 585 nm. The excitation wavelength in the PL locates at a shorter wavelength. This can be attributed to the Stokes shift. It means significantly different wavelengths for the excitation and emission of the (0; 0) transitions, which occurs if the potential functions of the π-electron system are different in the ground and excited states. In

the prepared sample, it can be considered that the interactions between the SBA-15 host and the RhB gust are strong, causing variations of bond distances and decreases of the perfection of conjugation in the RhB molecule. Further, the increased probabilities for (0; 1) transitions occur frequently for the distorted RhB in the pores of SBA-15. These properties result in the above phenomena.

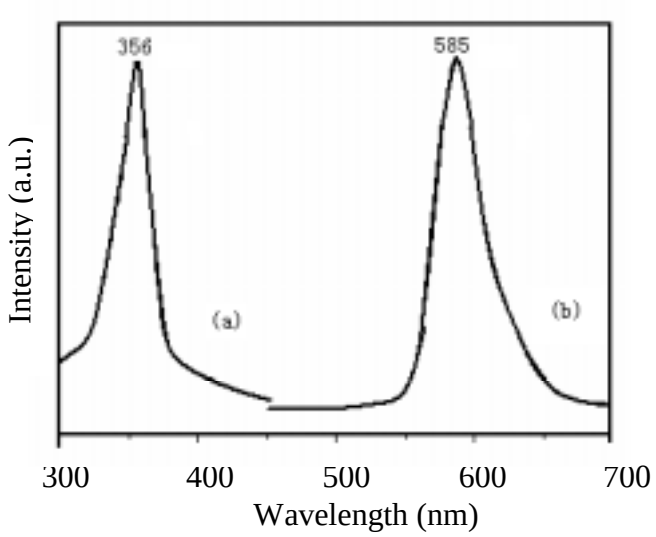

Fig. 7. Luminescence spectra of the samples: (a) excitation spectrum (λ_{em} = 585 nm); (b) emission spectrum (λ_{ex} = 356 nm)

Conclusion

The host-guest nanocomposite material (SBA-15)-RhB was prepared by liquid grafting method. Combined results of chemical analysis, powder XRD, FTIR, UV-Vis diffuse reflectance absorption spectroscopy, low temperature N_2 adsorption-desorption technique and photoluminescence studies have proved that the RhB nanoparticles were confined inside the pores of the SBA-15 and that the hexagonally ordered mesostructure of SBA-15 is remained and the host-guest nanocomposite material (SBA-15)-RhB shows luminescence. The obvious blue-shifts in the UV-Vis absorption spectra are attributed to the confinement of channels of the SBA-15 host on the guest and present the quantum size effects of the nanosized rhodamine B. The photoluminescence studies showed that the strong interaction between the SBA-15 host and the RhB guest exists, causing variations of bond distances and decreases of the perfection of conjugation in the RhB molecules. The prepared host-guest nanocomposite material (SBA-15)-RhB possesses luminescence performance and may be used as luminescence materials.

REFERENCES

1. C.T. Kresge, M.E. Leonwicz, W.J. Roth, J.C.Vartuli and J.S. Beck, *Nature*, **359**, 710 (1992).
2. J.S. Beck, J.C. Vartuli, W.J. Roth, M.E. Leonowicz, C.T. Kresge, K.D. Schmitt and T.W. Chu, *J. Am. Chem. Soc.*, **114**, 10834 (1992).
3. G.D. Stucky and J.E. Mac Dongall, *Science*, **274**, 669 (1990).
4. X.S. Zhao, G.Q. Lu and G.J. Millar, *Ind. Eng. Chem. Res.*, **35**, 2075 (1996).
5. A. Corma, *Chem. Rev.*, **97**, 2373 (1997).
6. U. Ciesla and F. Schuth, *Micropor. Mesopor. Mater.*, **27**, 131 (1999).
7. E.D. Davis, *Nature*, **417**, 813 (2002).
8. H. Yu and Q.Z. Zhai, *Bull. Chin. Ceram. Soc.*, **25**, 123 (2006).
9. F. Marlow, J. Caro, L. Werner, J. Kornatowski and S. Dahne, *J. Phys. Chem.*, **97**, 11286 (1993).
10. K. Hoffmann and F. Marlow, *J. Caro, Adv. Mater.*, **9**, 567 (1997).
11. U. Vietze, O. Krauss, F. Laeri, G. Ihlein, F. Schuth, B. Limburg, M. Abraham, *Phys. Rev. Lett.*, **81**, 4628 (1998).
12. I. Braun, G. Ihlein, F. Laeri, J.U. Nockel, G. Schulz-Ekloff, F. Schuth, U.Vietze, O. Weiss and D. Wohrle, *Appl. Phys. B*, **70**, 335 (2000).
13. D.E. De Vos and P.A. Jacobs, *Stud. Surf. Sci. Catal.*, **137**, 957 (2001).
14. Y. Rohlfing, D. Wohrle, M. Wark, G. Schulz-Ekloff, J. Rathousky and A. Zukal, *Stud. Surf. Sci. Catal.*, **129**, 295 (2000).
15. B.J. Scott, G. Winsberger and G.D. Stucky, *Chem. Mater.*, **13**, 3140 (2001).
16. G. Schulz-Ekloff, D. Wohrle, B.V. Duffel and R.A. Schoonheydt, *Micropor. Mesopor. Mater.*, **51**, 91 (2002).
17. R. Reisfeld, *Opt. Mater.*, **4**, 1 (1994).
18. H.S. Zhou, H. Sasabe and I. Honna, *J. Mater. Chem.*, **8**, 515 (1998).
19. C.E. Fowler, S. Mann and B. Lebeau, *Chem. Commun.*, **17**, 1825 (1998).
20. B. Lebeau, C.E. Fowler, S.R. Hall and S. Mann, *J. Mater. Chem.*, **9**, 2279 (1999).
21. N.K. Mal, M. Fujiwara and Y. Tanaka, T. Taguchi and M. Matsukata, *Chem. Mater.*, **15**, 3385 (2003).
22. D.M. Li, W.J. Zhao, X.D. Sun, J.L. Zhang, M. Anpo, J.C. Zhao, *Dyes Pigments*, **68**, 33 (2006).
23. D.Y. Zhao, J. Feng, Q. Huo, N. Melosh, G.H. Fredrickson, B.F. Chmelka and G.D. Stucky, *Science*, **279**, 548 (1998).
24. D.Y. Zhao, Q. Huo, J. Feng, B.F. Chmelka and G.D. Stucky, *J. Am. Chem. Soc.*, **120**, 6024 (1998).
25. M.H. Huang, A. Choudrey and P.D. Yang, *Chem. Commum.*, 1063 (2000).
26. Y. Han, J.M. Kim and G.D. Stucky, *Chem. Mater.*, **12**, 2068 (2000).
27. Y.J. Han, G.D. Stucky and B. Alison, *J. Am. Chem. Soc.*, **121**, 9897 (1999).
28. J.W. Zhao, F. Gao, Y.L. Fu, W. Jin, P.Y. Yang and D.Y. Zhao, *Chem. Commun.*, 752 (2001).
29. Q.Z. Zhai and C.Y. Mei, *Hydrometallurgy of China*, **4**, 56 (1998).
30. S. Brunauer, P.H. Emmett and E. Teller, *J. Am. Chem. Soc.*, **60**, 309 (1938).
31. E.P. Barrett, L.G. Joyner and P.P. Halenda, *J. Am. Chem. Soc.*, **73**, 373 (1951).
32. K.S.W. Sing, D.H. Everett, R.A.W. Haul, L. Moscow, R.A. Pierotti, J. Rouquerol and T. Siemieniewska, *Pure. Appl. Chem.*, **57**, 603 (1985).

(*Received*: 14 April 2008; *Accepted*: 17 November 2008) AJC-7046